Pharmaceutical Sciences Asia

Pharm Sci Asia 2026; 53(1), 23-36

DOI:10.29090/psa.2026.01.25.4781

Research Article

LC–MS/MS metabolite profiling and *in vivo* antidiabetic, antilipidemic, and hepatoprotective potential of *Ipomoea mombassana* leaf extract with *in silico* validation

Lakshmi Rajita. Kotta, A.Vijayalakshmi*

Department of Pharmacognosy Analysis, School of Pharmaceutical Sciences, Vels Institute of Science, Technology and Advanced Studies, Pallavaram-600117, Chennai, Tamil Nadu, India.

ABSTRACT

Diabetes mellitus, often associated with dyslipidemia and hepatic dysfunction, requires effective plant-derived therapeutics. This study evaluated the metabolite profile and pharmacological potential of the ethanolic leaf extract of *Ipomoea mombassana* Vatke (IMLE). LC-MS/MS profiling identified 37 phytochemicals, including flavonoids, alkaloids, terpenoids, and two previously unreported compounds, zinnimidine and cinncassiol A 19-glucoside. Molecular docking demonstrated strong inhibitory activity of key metabolites against α-amylase, with binding energies ranging from -7.6 to -9.8 kcal/mol. Tephrosin exhibited the most favorable binding (-9.8 kcal/mol), stabilized by hydrogen bonds with HIS305 (74.9% occupancy) and TRP59 (52.2%). Molecular dynamics simulations (100 ns) confirmed complex stability, with protein RMSD ~0.18 nm, ligand RMSD 0.04-0.07 nm, and average MMGBSA free energy –50.73 kcal/mol. *In vivo*, IMLE (200 mg/kg) significantly reduced fasting blood glucose from 344 ± 1.6 to 180 ± 3.9 mg/dL (≈48%; $p<0.001$), comparable to metformin (175 ± 7.1 mg/dL), and improved oral glucose tolerance. Dyslipidemia was corrected, with total cholesterol reduced by 38%, triglycerides by 35%, LDL-C by 68%, and HDL-C increased by 79% (all $p<0.001$). Elevated SGOT and SGPT were reduced (71 → 42 U/L; 87 → 51 U/L; $p<0.001$). Antioxidant markers (SOD, CAT, GSH) increased ~3-fold, while MDA decreased ~65% ($p<0.001$). Histopathology confirmed reversal of pancreatic and hepatic damage. Overall, integrated LC-MS/MS profiling, docking, molecular dynamics, and *in vivo* studies establish *I. mombassana* as a promising candidate for the management of diabetes and associated metabolic disorders.

Keywords:
Ipomoea mombassana; LC-MS/MS; Tephrosin; Antidiabetic activity; Antilipidemic activity; Hepatoprotective effect; Molecular docking; Molecular dynamics simulation

1. INTRODUCTION

Diabetes mellitus (DM) is a chronic condition involving impaired glucose, protein, and lipid metabolism. It often includes varying levels of insulin resistance and increases the risk of cardiovascular and other vascular complications. Hereditary and surroundings contribute to its onset[1]. Despite associated adverse effects such as insulin resistance, fatty liver, brain shrinkage, and anorexia nervosa, insulin therapy remains the primary option for diabetes [2-3].

Ipomoea mombassana Vatke, which belongs to the genus of Ipomoea from the Convolvulaceae family, its primary distribution is in tropical and warm temperate regions across the world. This taxon was first collected and named in Mombasa, Kenya in 1882, and it is prevalent

***Corresponding author:**
* A.Vijayalakshmi Email: vlakshmi.sps@velsuniv.ac.in

Pharmaceutical Sciences Asia © 2024 by
Faculty of Pharmacy, Mahidol University, Thailand is licensed under CC BY-NC-ND 4.0. To view a copy of this license, visit https:// www.creativecommons.org/licenses/by-nc-nd/4.0/

prevalent in Kenya's coastal areas[4]. Biju later discovered this species in the dry deciduous woods of Chinnar in Kerala, India[5]. In Telangana State, the genus *Ipomoea* has been reported to comprise 18 species according to Pullaiah[6] et al., whereas Reddy[7] et al., recorded 14 species. Ipomoea is a genus of plants that has long been used in traditional medicine to treat a number of clinical disorders processes [8]. *Ipomoea mombassana Vatke* is a new distribution record for the flora of Telangana State, India[9].

Despite the absence of scientific research on the pharmacological and phytochemical properties of *Ipomoea mombassana* Vatke, examining related species within the *Ipomoea* genus can provide valuable insights. For instance, *Ipomoea digitata* has been reported to possess a wide range of pharmacological activities, including anti-diabetic, antioxidant, hepatoprotective, and galactagogue effects, attributed to the presence of flavonoids, phenolic acids, alkaloids, saponins, and tannins[10]. Similarly, *Ipomoea carnea* has demonstrated potential against diseases such as cancer, diabetes, and inflammation, with its chemical constituents including 2-ethyl-1,3-dimethylbenzene, hexadecanoic acid, and linoleic acid[11]. Furthermore, a comparative phytochemical study found alkaloids, tannins, and steroids in various parts of *Ipomoea* species, indicating the genus's rich phytochemical profile[12]. As far as we know, no scientific research has been conducted specifically on the pharmacological or phytochemical properties of *Ipomoea mombassana* Vatke. This study aims to fill this gap by evaluating the bioactive potential of its leaves. When analyzing plant-derived phytochemicals or activities, careful consideration of extraction solvents and components is critical[13]. The primary objective of this study was to investigate the antidiabetic and antioxidant potential of the ethanolic leaf extract of *Ipomoea mombassana* (IMLE) through a combination of *in vitro*, *in vivo*, and metabolite profiling approaches. The α-amylase inhibition assay was specifically chosen as the *in vitro* model because excessive postprandial glucose release from starch hydrolysis is a hallmark of type 2 diabetes, and inhibition of α-amylase is a well-established therapeutic strategy to delay carbohydrate digestion and attenuate hyperglycemia[14].

Secondary metabolites, including alkaloids, flavonoids, terpenoids, and phenolics, are bioactive compounds that play key roles in plant defense, signaling, and environmental adaptation, and they also hold considerable clinical and commercial value. Liquid chromatography-mass spectrometry (LC-MS) is widely applied for their identification and characterization, as it couples the separation efficiency of liquid chromatography with the sensitivity of mass spectrometry to detect complex metabolite mixtures even at trace levels. Through accurate mass measurement, fragmentation profiling, and database comparison, LC-MS enables structural elucidation and supports metabolomics approaches for exploring metabolic changes and discovering novel bioactive compounds, thereby advancing natural product research and plant-based medicine[15-16]. Metabolomics, the comprehensive analysis of small molecules in biological samples, frequently employs untargeted LC-ESI-MS combined with chemometric data analysis[14]. Quadrupole time-of-flight (QTOF) analyzers are especially suited for such applications due to their high scan rate, mass accuracy, and ability to generate detailed MS/MS spectra[15]. Consequently, LC-ESI-QTOF-MS/MS metabolomics with chemometrics has been successfully used in food quality control, as demonstrated in studies on tomatoes and *Pinus* species[16].

Molecular docking and dynamics simulations are widely used in modern drug discovery to predict ligand–receptor interactions and assess binding stability[17]. Recent studies highlight their utility in phytochemistry-based drug discovery, especially for identifying natural antidiabetic agents [18-19]. In the present work, docking was performed to evaluate interactions of *Ipomoea mombassana* metabolites with α-amylase, α-glucosidase, HMG-CoA reductase, and Keap1, complementing *in vitro* assays. To refine docking predictions, molecular dynamics (MD) simulations and MM-GBSA free-energy calculations were carried out to assess the stability and energetics of high-affinity ligand–receptor complexes[20].

Streptomyces achromogenes produces the glucosamine-nitrosourea compound STZ, used in anticancer therapy. According to Lenzen (2008)[21], STZ-induced diabetes causes pancreatic β-cell degeneration and necrosis. This screening method considers traditional medicines known for effectively managing diabetes. Natural products play a key role in drug development, offering diverse lead compounds. Traditional medicine utilizes various organisms with broad pharmacological and therapeutic effects. Herbs, rich in phytochemicals, are a major source of potent medicinal agents and help reduce health risks[22].

2. MATERIALS AND METHODS

2.1. Materials

2.1.1. Collection of plant material, chemicals and drugs

In August 2023, plant samples of *Ipomoea mombassana* Vatke, belonging to the Convolvulaceae family, were collected from the wastelands of Palamkula village in the Ranga Reddy district of Telangana State, India. The plant was identified using available literature and authenticated under voucher number OUAS-148 by Dr. A. Vijaya Bhasker Reddy, Assistant Professor in the Department of Botany at the University College of

Science, Osmania University, Hyderabad, Telangana State, India. Ethanol from Bio Liqua Research Pvt Ltd, Bangalore, India. N-hexane, Ethyl acetate, and chloroform from Molychem Mumbai, Maharashtra India. Streptozotocin, Metformin from Sigma-Aldrich Banglore India.

2.1.2. Animals

All experimental protocols were approved by the IAEC having approval number CCSEA/IAEC/JLS/21/04/017. Male Wistar rats, weighing between 160 and 200 g on average and 7 weeks old, were randomly assigned to five treatment-based groups, each with six animals. Every animal was maintained on a 12-hour light/dark cycle and housed in a temperature-controlled room (22–24˚C) under safe laboratory conditions[23-25].

2.2. Soxhlet extraction process

Dried, powdered leaves of *Ipomoea mombassana* were Soxhlet-extracted successively with n-hexane, chloroform, ethyl acetate, and ethanol (low to high polarity). For each solvent, 100 g of leaf powder was loaded into a cellulose thimble and extracted with 500 mL solvent (leaf:solvent 1:5, w/v) at 60-65 °C for 6-8 h (10-12 siphon cycles), until the siphoning solvent became colorless. Crude extracts were concentrated under reduced pressure (rotary evaporator, 40 °C) and dried to constant mass in a vacuum oven (40 °C). Percentage yield was calculated as

$$\%yield = \frac{mass\ of\ dry\ extract\ (g)}{mass\ of\ dry\ plant\ material\ (g)} \times 100$$

2.3. Phytochemical analysis

Phytochemical screening of IMLE was performed using standard methods (Harborne, 1998) [26]. The extract was tested for alkaloids (Mayer's and Dragendorff's tests), carbohydrates (Molisch's test), glycosides (Keller–Killiani test), saponins (frothing test), proteins (Biuret test), phytosterols (Liebermann–Burchard test), terpenoids (Salkowski test), fixed oils (spot test), phenolics (ferric chloride test), flavonoids (Shinoda test), and tannins (gelatin test).

2.4. *In vitro* studies

The *in vitro* α-amylase inhibition assay was carried out using the DNSA (3,5-dinitrosalicylic acid) method. Briefly, different concentrations of IMLE (100-500 µg/mL) were incubated with 500 µL of α-amylase enzyme solution (1 U/mL in 0.02 M phosphate buffer, pH 6.9) at 37 °C for 10 min. After incubation, 500 µL of 1% starch solution (prepared in the phosphate buffer) was added as substrate and the mixture was further incubated at 37 °C for 15 min. The reaction was stopped by adding 1 mL of DNSA reagent, followed by boiling at 90 °C for 10 min and cooling to room temperature. The absorbance was measured at 540 nm using a UV-Vis spectrophotometer. Acarbose was used as a standard reference inhibitor. The percentage inhibition was calculated relative to the control (enzyme + substrate without extract), and IC_{50} values were determined from dose-response curves[27].

2.5. LC/MS/MS metabolite profiling of ethanolic extract of IMLE.

High-resolution LC-MS analysis was performed at the Sophisticated Analytical Instrument Facility (SAIF), Indian Institute of Technology (IIT) Bombay. The ethanolic extract sample is analyzed using an LC-MS system with a spectral library for impurity profiling and metabolite identification. An Agilent 1290 Infinity II LC system linked to an Agilent 6550 iFunnel Q-TOF mass spectrometer equipped with an electrospray ionization (ESI) source working in positive ion mode was used to perform the liquid chromatography-mass spectrometry (LC-MS). The Agilent Infinity Lab Poroshell 120 EC-C18 column (3.0 × 100 mm, 2.7 µm) was utilized for chromatographic separation in a G1316C thermostat column compartment at 40°C. The mobile phase was composed of 0.1% formic acid in water (solvent A) and acetonitrile (solvent B), with gradient elusion at a flow rate of 0.3 mL/min as follows: 5% B at 0 min, rising to 100% B at 25 min, holding for 5 min, and re-equilibrated to 5% B at 35 min. The injection volume was 5.0 µL, with the maximum system pressure set at 1200 bar.

Mass spectrometric detection was carried out in AutoMS/MS mode throughout a mass range of 120-1200 m/z. The MS and MS/MS scan rates were set to 1 spectrum per second, with the collision energy increased from 15 to 50 eV. The ionization source parameters were the gas temperature of 250°C, sheath gas temperature of 300°C, gas flow of 13 L/min, sheath gas flow of 11 L/min, and nebulizer pressure of 35 psi. The capillary and nozzle voltages were set at 3500 and 1000 volts, respectively. Precursor ions were chosen based on their abundance, with active exclusion enabled to prevent repetitive fragmentation of dominating ions. Data gathering and processing were accomplished using Agilent. Agilent MassHunter Workstation Software (Agilent Technologies, USA) was used for data acquisition and processing. Peak detection, spectral matching, and metabolite identification were carried out using the METLIN metabolite database and the Agilent Personal Compound Database and Library (PCDL), which provide accurate mass information and MS/MS spectral libraries for compound annotation[28].

2.6. *In silico* studies of ethanolic extract IMLE

Molecular dynamics simulations were performed using GROMACS 2022.2 with the CHARMM27 force field for protein topology, while ligand topology was generated using SwissParam. The protein–ligand system was solvated in a TIP3P water model, neutralized with Na^+ ions, and energy-minimized using the steepest descent algorithm. Equilibration was carried out with 100 ps NVT and 100 ps NPT simulations at 300 K and 1 bar, followed by a 100 ns production run under isothermal–isobaric conditions. Stability and binding affinity were evaluated through RMSD, RMSF, hydrogen bonding, MMGBSA binding free energy, radius of gyration (Rg), and solvent accessible surface area (SASA). Trajectories were analyzed using VMD and HeroMDAnalysis [29]. LC-MS/MS metabolite profiling was performed using Agilent Mass Hunter Workstation, with compound identification supported by METLIN [30] and Agilent PCDL databases. Molecular docking studies were conducted using AutoDock Vina [31], and docking results were validated through MD simulations.

2.7. *In vivo* studies of ethanolic extract IMLE.

2.7.1. Acute toxicity studies

Ipomoea mombassana Vatke leaf ethanolic extract (IMLE) was given orally to the mice in five groups at varying dosages (50–2000 mg/kg body weight). Group I served as normal control which received the vehicle, Group II served as diabetic control, Group III and IV served as tests group, receiving 100 and 200 mg/kg b.w. of IMLE respectively whereas Group V served as standard which received Metformin (100 mg/kg b.w.). Their behavior was closely watched for the first hour, and then often observed over the next 14 days. Safety was assessed by monitoring general behavior (alertness, grooming, locomotion, posture), neurological signs (tremors, convulsions, sedation), autonomic responses (salivation, piloerection, respiration), body weight, food and water intake, and mortality. Environmental conditions were maintained at 25 ± 2 °C with relative humidity of 45–55% and a 12 h light/dark cycle. The animals were housed in polypropylene cages, provided with a standard pellet diet, and allowed free access to water. No mortality was observed during the study, and the doses of 100 and 200 mg/kg were selected for subsequent pharmacological evaluation[32].

2.7.2. Induction of diabetes

At the start of the experiment, all rats had to fast for six to eight hours before receiving the injection of Streptozotocin (STZ). During this period, there were no limitations on the quantity of water available. Weighing out a volume of 32.5 mg of STZ, the material was divided into individual 1.5 mL microcentrifuge tubes and sealed with aluminum foil. To make the citrate buffer, one of these tubes was reserved for each rat. Prior to injection, the medication was dissolved in 50 mM sodium citrate buffer at a pH of 4.5 to yield 32.5 mg/mL of STZ. Using a 1-mL syringe and a 23-G needle, the STZ solution was injected intraperitoneally (i.p.) at a dose of 65 mg/kg (2.0 ml/kg) for the study groups (Donovan & Brown, 2006). An equivalent volume of citrate buffer was intraperitoneally administered into the control group. After being returned to their cages, the rats were fed their usual food and given 10 % sucrose water. On the second day of the experiment, 10 % sucrose water was replaced with regular water.

The rats were split up into seven groups: Group I was the normal control group, receiving the vehicle; Group II was the diabetic control group; Groups III and IV were the test groups, receiving 100 and 200 mg/kg body weight of IMLE; and Group V was the standard group, receiving 100 mg/kg body weight of Metformin. For 21 days, the medication was administered every day, and blood was drawn from the tail to measure blood glucose[33].

2.7.3. Body weight and serum analysis

Over the course of the treatment, the body weights of every animal were regularly monitored. Fasting blood glucose levels were measured by collecting blood from the tip of the tail vein. Glucose levels were determined using a portable glucometer (OneTouch® Basic, Lifescan Inc., USA) with glucose oxidase-based test strips, according to the manufacturer's instructions.

Using ether to induce unconsciousness, blood was extracted from the retro-orbital sinus of the animals on the twenty-first day of the treatment. The serum was separated ten minutes after collection using centrifugation at 10,000 g. Using diagnostic tools, the levels of triglycerides (TG), total cholesterol (TC), and high-density lipoprotein cholesterol (HDLc) in this serum were subsequently discovered. In addition, Datta et al. (2013)[34] used Friedwald's algorithm to calculate the levels of low-density lipoprotein cholesterol (LDLc) and very low-density lipoprotein cholesterol (VLDLc). Additionally, using diagnostic kits, the levels of glutamic-oxaloacetic transaminase and glutamic pyruvic transaminase in serum were determined. Superoxide dismutase (SOD), reduced glutathione (GSH), catalase, and malondialdehyde (MDA) were among the antioxidants whose levels were estimated from the serum.

Table 1. Qualitative Phytochemical Screening of IMLE

Phytochemical class	Test performed	Observation (colour change / precipitate)	Inference
Alkaloids	Mayer's test	Cream/white precipitate	+
Flavonoids	Shinoda test	Pink/red colour	+
Tannins/Phenolics	Ferric chloride test	Blue-green/black colour	+
Saponins	Froth test	Stable froth formation	+
Terpenoids	Salkowski test	Reddish-brown colour at interface	+
Glycosides	Keller–Killiani test	Brown ring at interface	+
Steroids	Liebermann–Burchard test	Blue-green colour	+
Proteins	Biuret test	Violet colour	+
Carbohydrates	Molisch's test	Violet ring at interface	+

(+ = present; – = absent, if you observed absence for some groups)

2.8. Histopathological studies

Histopathological analyses were performed on the last day of the experiment. Following its removal and preservation in 10 % formaldehyde, the pancreas was imbedded in paraffin. The preserved tissues were used to cut sections using a microtome (Finesse 325, Thermo Scientific, Runcorn, UK) that measured 3-5 µm. These sections were then mounted on glass slides. Histological investigations were carried out at 200 and 400x magnifications using hematoxylin and eosin (H&E) staining, in accordance with the methodology described by Nagy and Ewais[35].

2.9. Statistical analysis

Graph pad prism was used to do statistical analyses. The statistically significant differences across all groups were examined using an ANOVA test. Differences were deemed significant when the p-value was less than 0.05, and the Tukey's test was utilized for this purpose.

3. RESULTS

3.1. Phytochemical analysis

Preliminary phytochemical analysis of the ethanol leaf extract revealed (Table 1) the presence of various bioactive compounds. The extract tested positive for carbohydrates, glycosides, saponins, terpenoids, phenolic compounds, flavonoids, and tannins.

3.2. Alpha amylase activity of ethanolic extract of *Ipomoea mombassana* leaves

The ethanolic extract demonstrated significant inhibition of amylase activity, with the percentage inhibition observed across different concentrations. The IC50 value for the ethanolic extract was determined to be 45 ± 1.7 µg/mL, indicating a substantial inhibitory effect on the enzyme.

3.3. LC-MS analysis revealing phytochemical composition of ethanolic extract

High Resolution- Liquid Chromatography Mass Spectrometry (HR-LCMS) was carried out on the chemical composition of the active ethanolic extract. This technique was performed in the separation and identification of the phytoconstituents based on their retention times (RT), molecular formulas, accurate mass-to-charge ratios (M+H] m/z), and MS/MS fragmentation patterns, database difference (library) and mode of action with references. MS data were provided in positive ionization mode. Most of the m/z values in our extract were in the range of 146 to 593. LC–QTOF–MS/MS analysis of IMLE revealed 37 identified compounds (Table 2). The corresponding chromatogram is shown in Figure 1, where only identified peaks are labeled, while impurity or background peaks remain unassigned. The identified metabolites were structurally diverse, including amino acid derivatives (e.g., GLU-VAL, L-isoleucyl-L-proline, Valyl-Glycine, Valyl-Valine), alkaloids (e.g., Pilocarpine, Abrine, Zinnimidine), dipeptides, flavonoid derivatives such as Tephrosin, and terpenoids such as Ganoderic acid. Other notable compounds included Piperolein B, XE991, and Bis-γ-glutamylcystine. This structural diversity is consistent with the broad phytochemical classes detected in preliminary qualitative screening (Table 1). The phytochemical constituents of *Ipomoea mombassana* leaf extract (IMLE) were characterized based on LC–MS spectral data and chemical structure analysis (Figure S1).

Although the dominant chromatographic peaks at RT 1.82, 9.08, 9.80, and 19.37 min correspond to abundant metabolites such as 11-amino-undecanoic acid, (S)-Edulinine, 6'-Dehydro-6'-oxyparomamine, and Methyl-2-furoate, these compounds are not reported in the literature as antidiabetic or antioxidant agents. Importantly, peak intensity reflects relative abundance and does not necessarily predict pharmacological activity. Instead, structurally relevant metabolites detected at lower abundance such as Tephrosin,

Table 2. Compounds identified in ethanolic extract of *Ipomoea mombassana* leaves by LC–QTOF–MS/MS. Only identified compounds are listed; impurity/background peaks observed in the chromatogram were excluded.

S.no	Retention time (min)	[M+H] *(m/z)*	Error (ppm)	Molecular formula	MS/MS Fragment Ions *(m/z)*	Identification	Phytochemical class
1	1.82	202.1	12.3	C11H23NO2	142.12	11-amino-udecanoic acid	Others
2	1.84	269.1	8.3	C10H18N2O5	136.05, 233.08	GLU-VAL	Peptides / Dipeptides
3	2.05	229.15	15.7	C11H20N2O3	142.08	L-isoleucyl-L-proline	Peptides / Dipeptides
4	2.11	185.04; 241.15;	1.3; 14.0; -	C6H10O5; C12H20N2O3	167.03; 196.09, 121.07	L-Rhamnono-1,4-lactone; Pirbuterol	Others
5	2.12	344.22	2.2	C21H29NO3	181.1, 118.08	Piperolein B	Alkaloid
6	4.50	188.06	-1.0	C9H11NO2	146.05, 118.06	Methyl N-methylanthranilate	Amino acid derivative
7	4.59	205.09	14.1	C11H12N2O2	188.06, 146.05	D-Tryptophan	Amino acid derivatives
8	4.83	287.15	-7.9	C18H20N2	115.08,	Mianserin	Synthetic tetracyclic alkaloid
9	4.89	146.05	-6.0	C7H9NO	118.06	2-Propionylpyrrole	Pyrrole derivative
10	5.14	317.11	-5.6	C19H18O3	155.06, 185.03	1-Methoxy-4[5-(4-methoxyphenoxy)-3-penten-1-ynyl]benzene (anisoles)	Flavonoids / Phenolics
11	5.31	175.10	14.1	C7H14N2O3	101.03	Valyl-Glycine	Peptides / Dipeptides
12	5.39	355.09	-2.8	C15H18N2O6S	163.03, 193.04	(S)-n-[3-3,4-Methylenedioxyphenyl)-2-(mercaptomethyl)-1-oxoprolyl]glycine.	Phenylpropanoid amide
13	5.58	433.12	-4.9	C23H22O7	127.03	Tephrosin	Flavonoids / Phenolics
14	5.94	231.10; 158.09	6.9; 1.4	C11H16N2O2; C9H13N	158.09; 143.07	Pilocarpine; 3-Butylpyridine	Alkaloids
15	6.03	251.09; 287.13; 273.11	6.4; 9.0; 4.8	C10H16; C14H20; C13H18N2O3	161.06, 215.07; 269.12, 209.10; 195.03, 255.1	Prolyl-Hydroxyproline; Valyl-Phenylalanine; 4-Coumaroyl-2-hydroxyputrescine	Peptides / Dipeptides
16	6.06	285.11	19.3	C11H16N4O5	269.12, 195.08	Glutamyl-histidine	Amino acid derivatives
17	6.59	283.10	1.3	C11H14N4O5	211.08, 167.05	1-Methylinosine	Nucleoside derivative
18	7.92	265.09	-5.3	C10H16O8	206.08, 247.08	3-Hydroxy-4-butanolide	Others
19	8.21	377.16	0.8	C26H20N2O	254.07	XE991	Alkaloids
20	8.28	499.11	-1.5	C16H26N4O10S2	163.03	Bis-γ-glutamylcystine	Peptide derivative
21	8.78	206.15	4.7	C11H21NO	165.11	Tecostanine	Amino acid derivatives
22	8.85	284.12	-6.3	C10H19N3O5	147.04, 121.06	Aspartyl-Lysine	Amino acid derivatives
23	9.08	314.13	7.4	C16H21NO4	177.05, 121.06	(S)-Edulinine	Alkaloids
24	9.33	284.12	9.3	C15H19NO3	147.04, 129.11	Zinnimidine	Alkaloids
25	9.34	567.23	2.1	C26H40O12	147.04	Cinncassiol A 19-glucoside	Terpenoids
26	9.80	344.14	-0.3	C12H23N3O7	177.05	6'-Dehydro-6'-oxyparomamine	Aminoglycoside
27	10.27	217.15	-2.2	C10H20N2O3	157.09	Valyl-Valine	Peptides / Dipeptides
28	10.34	241.09	8.6	C12H14N2O2	167.05	Abrine	Alkaloids
29	10.41	488.16	9.8	C26H27NO7	121.06	(E) -Squamosamide	Flavonoids / Phenolics
30	11.71	268.12	1.6	C12H17N3O4	121.02	L-Agaritine	Amino acid derivative

Table 2. Compounds identified in ethanolic extract of *Ipomoea mombassana* leaves by LC–QTOF–MS/MS. Only identified compounds are listed; impurity/background peaks observed in the chromatogram were excluded. (Continued)

S.no	Retention time (min)	[M+H] *(m/z)*	Error (ppm)	Molecular formula	MS/MS Fragment Ions *(m/z)*	Identification	Phytochemical class
31	12.93	318.29	-13.9	C20H35N3	256.25	Ormosanine	Alkaloids
32	19.37	149.02	-5.2	C6H6O3	121.02	Methyl2-furoate	Others
33	24.15	593.26	7.0	C32H42O9	533.24	Ganoderic acid	Terpenoids

Ganoderic acid, peptide derivatives, and phenolic compounds have well-documented antioxidant and antidiabetic activities. This observation, together with our *in vitro* results (α-amylase inhibition and antioxidant assays), suggests that the therapeutic potential of IMLE arises from these bioactive metabolites rather than from the most abundant peaks.

The fragmentation patterns (MS/MS ions) corroborated the structural identities of these metabolites, and their biological activities were estimated using spectrum matching and literature references.

3.4. Molecular dynamics simulation of tephrosin-α-amylase complex

Molecular dynamics (MD) simulations of the Tephrosin α-amylase complex were performed for 100 ns to evaluate its structural stability and binding interactions. The protein backbone RMSD stabilized after 15 ns and remained within 0.17-0.19 nm, while the ligand RMSD was maintained at 0.04-0.07 nm, indicating stable binding (Figure 2A). RMSF analysis showed limited residue fluctuations, with higher mobility at loop regions (residues 130-170 and 320-360), whereas active site residues remained stable (Figure 2B). Hydrogen bond analysis revealed 2-5 bonds during the trajectory, with an average of 3-4 stable interactions (Figure 3A). Occupancy analysis highlighted persistent bonding with HIS305 (74.9%) and TRP59 (52.2%) (Figure S2). Binding free energy (MMGBSA) was favorable, averaging -50.73 kcal/mol, with stabilization observed at 50 ns and 100 ns (Figure 3B). The compactness of the protein, assessed by radius of gyration (Rg), remained stable at 2.32-2.36 nm (Figure S3), while SASA values were consistent within 192–208 nm², indicating no major conformational changes (Figure 4).

3.5. Effect IMLE on body weight and serum glucose levels

3.5.1. Effect on body weight

The initial body weight across all animal groups was statistically comparable. However, induction of diabetes led to a significant reduction in body weight compared to the normal control group throughout the experimental period. This decline is attributed to

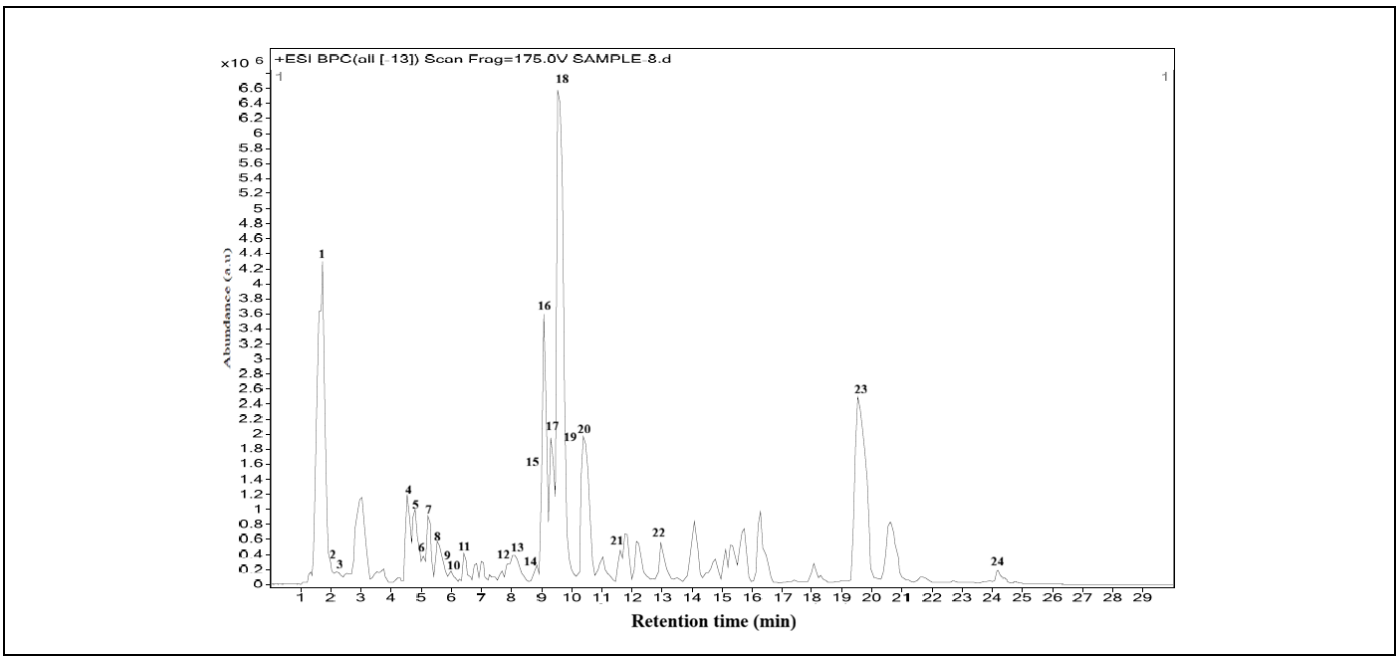

Figure 1. LC-QTOF-MS/MS chromatogram of ethanolic extract of *Ipomoea mombassana* leaves. Peaks are numbered according to compounds listed in Table 2. Only identified compounds are labeled, while unassigned impurity peaks are not annotated. X-axis: Retention time (min); Y-axis: Abundance (a.u.).

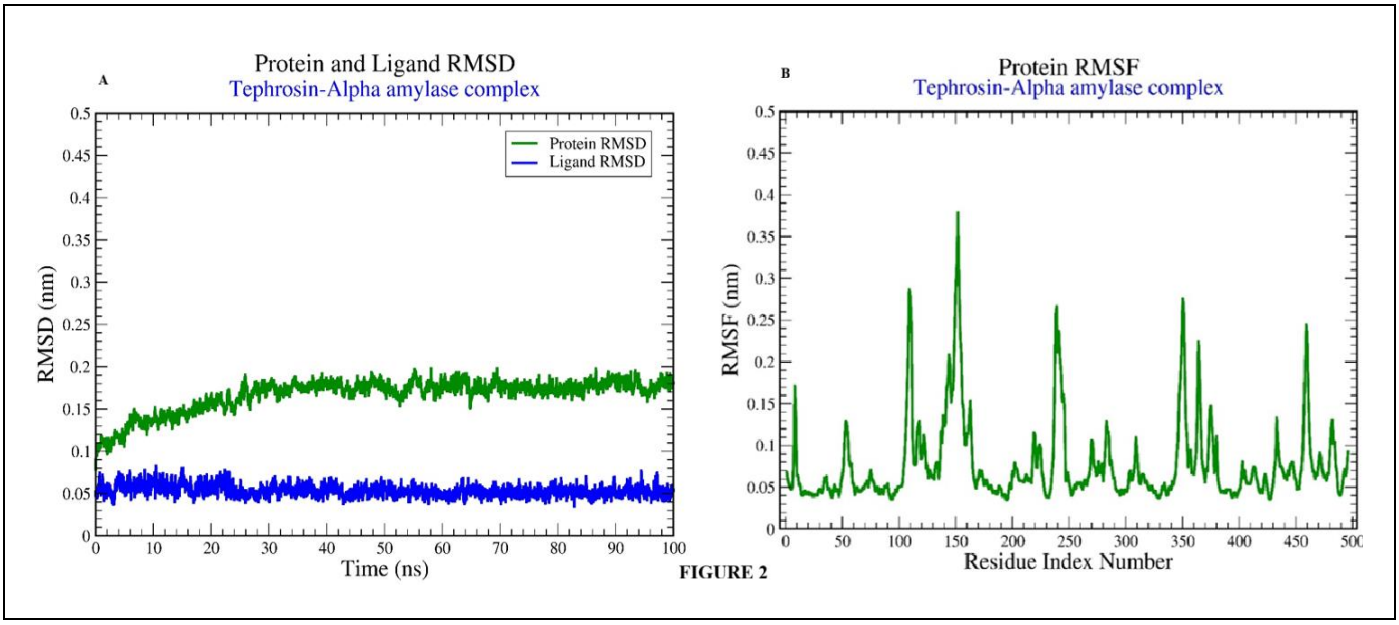

Figure 2. Molecular dynamics stability plots of Tephrosin-α-amylase complex during 100 ns simulation. (A) Root Mean Square Deviation (RMSD) of protein backbone (green) and ligand (blue), showing structural stability and consistent binding. (B) Root Mean Square Fluctuation (RMSF) analysis of α-amylase residues bound with Tephrosin. Most residues show minimal fluctuations, while loop regions exhibit higher flexibility. Active site residues remain stable, confirming ligand anchoring**.**

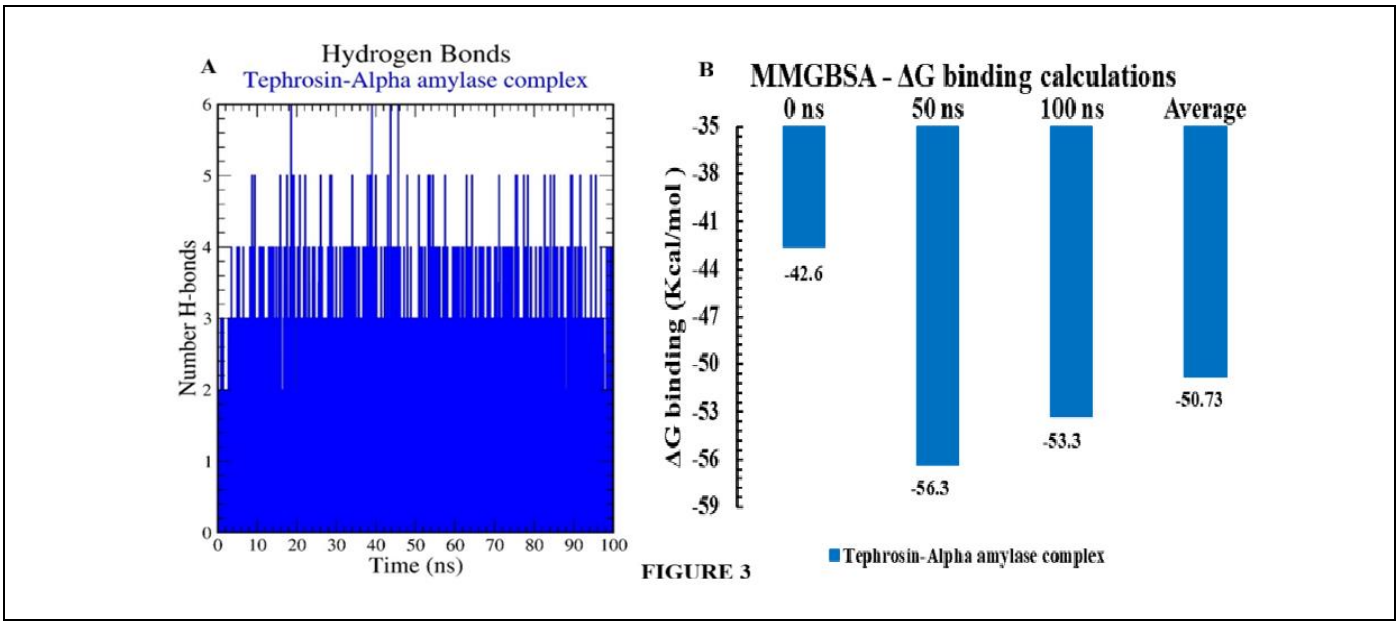

Figure 3. Molecular dynamics interaction profiles of Tephrosin -α-amylase complex. (A) Number of hydrogen bonds formed between Tephrosin and α-amylase during 100 ns MD simulation, showing stable 2-5 hydrogen bonds with an average of 3-4 throughout the trajectory. (B) Binding free energy (ΔG) calculated by MMGBSA at 0, 50, and 100 ns. The average ΔG (-50.73 kcal/mol) demonstrates thermodynamic stability and favorable protein-ligand interactions**.**

insufficient insulin activity, which restricts glucose utilization and promotes the breakdown of fat and muscle proteins, resulting in progressive weight loss. Treatment with IMLE at a dose of 100 mg/kg body weight produced a significant ($p < 0.001$) improvement in body weight compared to the diabetic control group. Furthermore, the reduced body weight was markedly ameliorated in all treatment groups ($p < 0.001$) when compared with the diabetic control group (Figure 5).

3.5.2. Effect on serum glucose level

Baseline serum glucose levels were comparable across all groups. The diabetic control (DC) group exhibited a significant rise from 92 ± 2.2 to 344 ± 1.6 mg/dL ($p < 0.001$ vs. normal control). All treatment groups significantly reduced serum glucose compared to DC ($p < 0.001$), demonstrating their effectiveness in managing hyperglycemia (Figure 6).

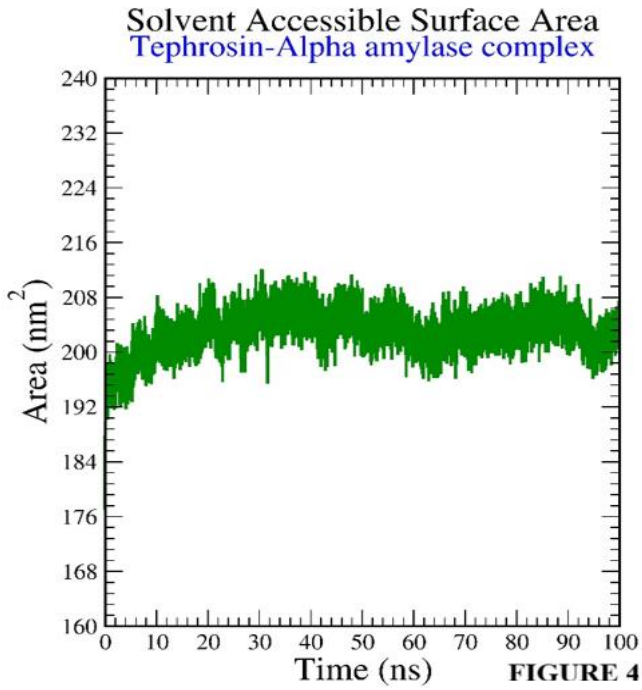

Figure 4. Solvent Accessible Surface Area (SASA) of α-amylase bound with Tephrosin during the 100 ns MD trajectory. The consistent SASA values (192-208 nm²) indicate compactness and absence of major conformational changes or unfolding upon ligand binding.

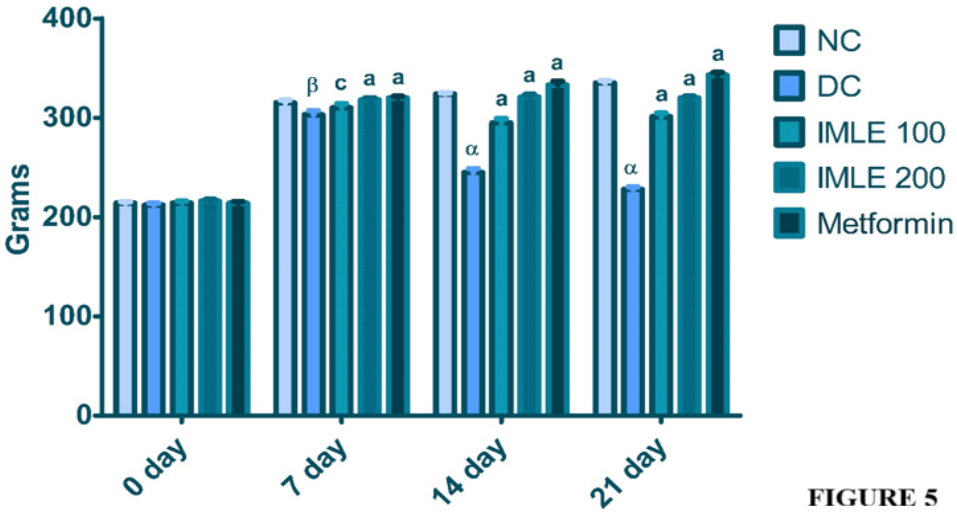

Figure 5. Effect of IMLE on body weight in experimental rats. Values are expressed as mean ± Standard Error of Mean (SEM), n = 6 in each group. $^{\alpha}p < 0.001$, $^{\beta}p < 0.01$ compared to the NC group; $^{a}p < 0.001$, $^{b}p < 0.01$, $^{c}p < 0.05$ compared to the DC group.

3.6. Effect of IMLE on oral glucose tolerance test

An oral glucose tolerance test (OGTT) was performed to evaluate glucose regulation in different treatment groups. The postprandial glucose area under the curve (PG-AUC) was calculated to quantify overall glucose exposure during the test. The mean OGTT levels of the NC group were 261 ± 6.5 mg /dL, which was significantly ($p < 0.001$) increased to 383 ± 2.5 mg/dL in the DC group. These increased levels were significantly decreased in the treatment groups ($p < 0.001$) (Figure 7).

3.7. Effect of IMLE on serum lipid profile

Diabetes induction resulted in significant alterations in the serum lipid profile compared to the normal control (NC) group. The mean serum total cholesterol level in the NC group was 89 ± 2.2 mg/dL,

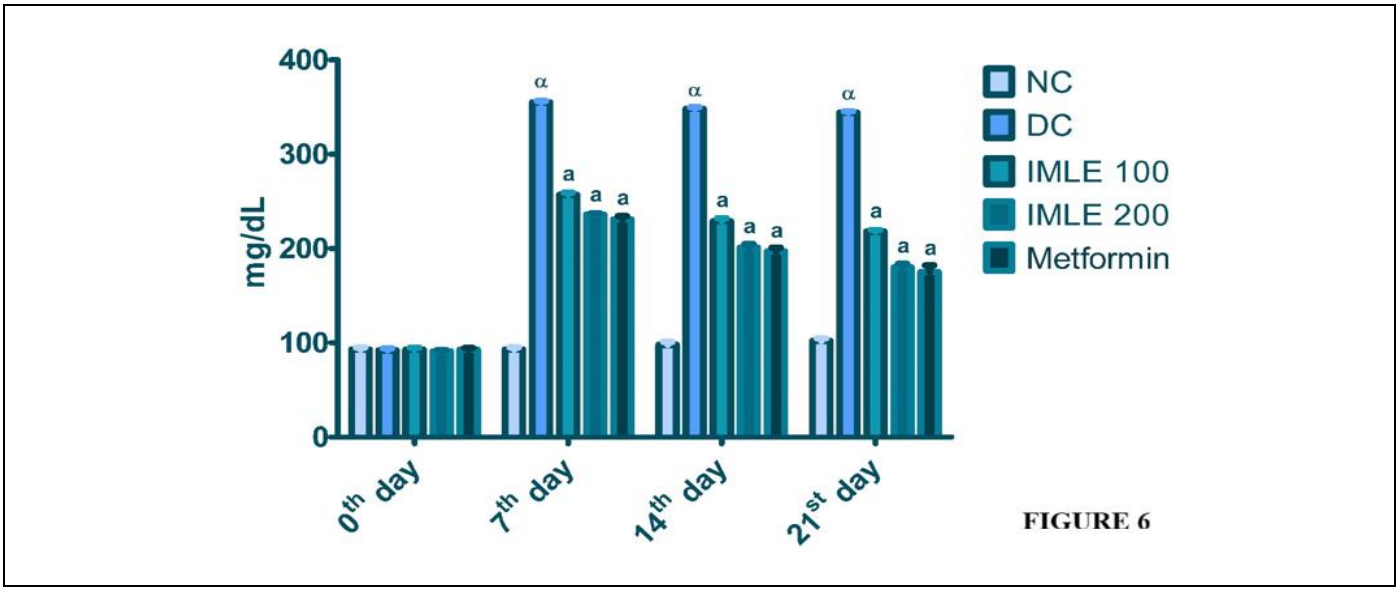

Figure 6. Effect of IMLE on serum glucose levels in experimental rats. Values are expressed as mean ± SEM, n = 6 in each group. $^{\alpha}p < 0.001$ compared to the NC group; $^{a}p < 0.001$ compared to the DC group**.**

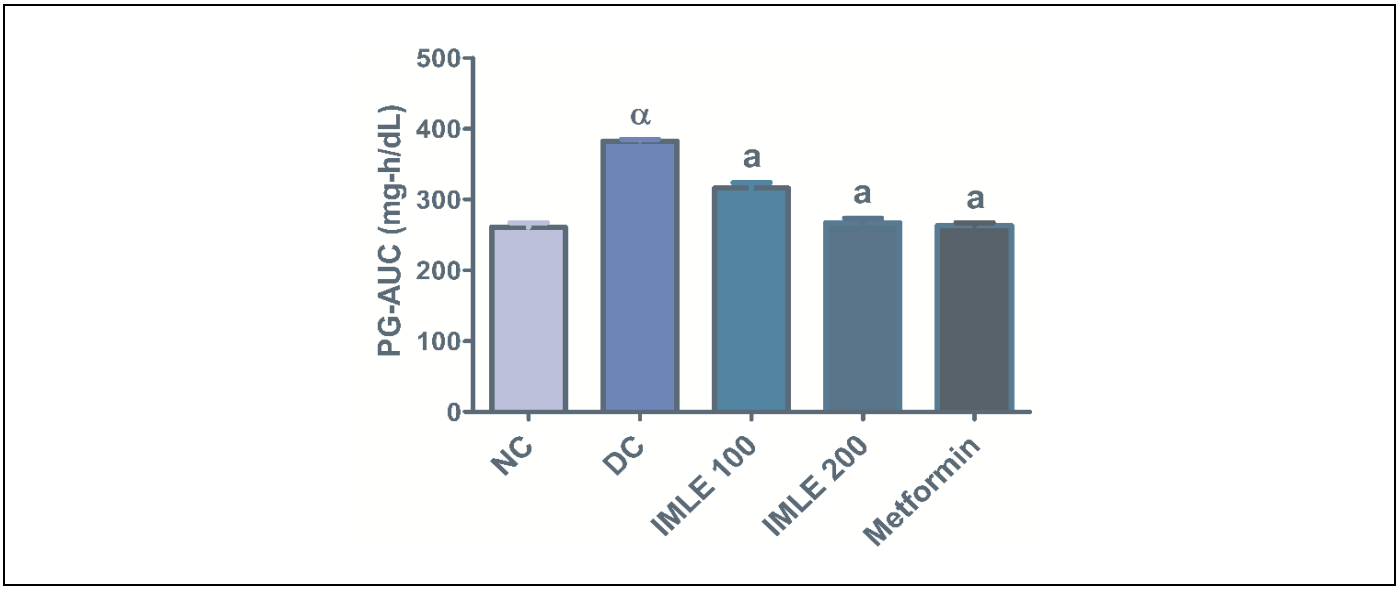

Figure 7. Effect of IMLE on oral glucose tolerance test (OGTT) and postprandial glucose area under the curve (PG-AUC) in experimental rats. Data were analyzed using one-way ANOVA followed by Tukey's test. $^{\alpha}p < 0.001$, $^{\beta}p < 0.01$ compared to the NC group; $^{a}p < 0.001$, $^{b}p < 0.01$, $^{c}p < 0.05$ compared to the DC group.

which increased significantly ($p < 0.001$) to 157 ± 2.4 mg/dL in the diabetic control (DC) group. Treatment with all extract and standard drug groups significantly reduced total cholesterol levels ($p < 0.001$). Similarly, serum HDL-cholesterol levels were markedly reduced in the DC group (19 ± 0.90 mg/dL) compared to the NC group (41 ± 1.4 mg/dL, $p < 0.001$). Treatment with IMSE 100, IMSE 200, and IMLE 100 showed a mild but significant increase in HDL levels ($p < 0.05$), while IMLE 200 and metformin significantly elevated HDL-c levels ($p < 0.001$) compared to the DC group. The serum LDL-c level was also significantly increased in the DC group (102 ± 1.1 mg/dL) compared to the NC group (29 ± 1.6 mg/dL, $p < 0.001$). All treatment groups demonstrated a significant reduction in LDL-c levels ($p < 0.001$). VLDL-c levels rose significantly from 20 ± 0.91 mg/dL in the NC group to 40 ± 1.1 mg/dL in the DC group ($p < 0.001$). Treatment with IMSE 200 ($p < 0.01$), IMLE 100 ($p < 0.05$), IMLE 200, and metformin ($p < 0.001$) significantly decreased VLDL-c levels, while IMSE 100 showed no significant change. Additionally, serum triglyceride levels increased significantly in the DC group (186 ± 2.5 mg/dL) compared to the NC group (97 ± 1.3 mg/dL, $p < 0.001$). This elevation was significantly reversed in all treatment groups ($p < 0.001$), indicating an overall improvement in the lipid profile following treatment. Data were analyzed by using one ANOVA followed by Tukey's Test. All the values are

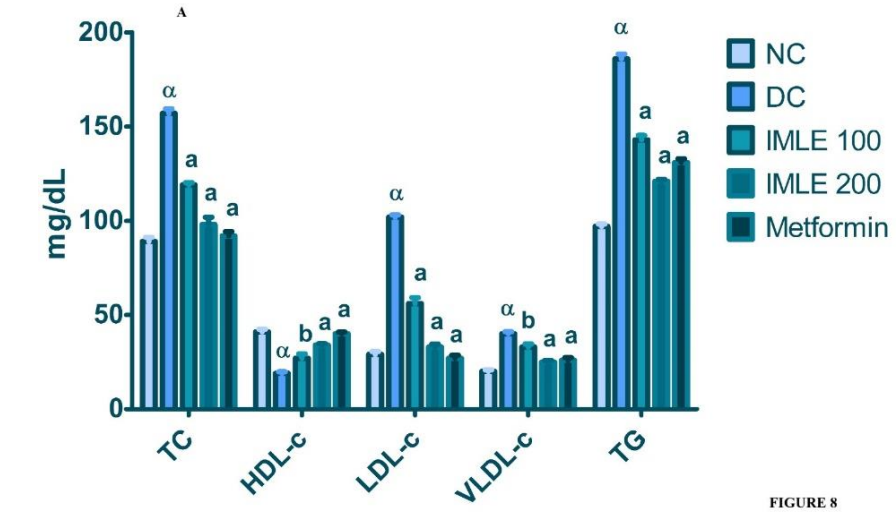

FIGURE 8

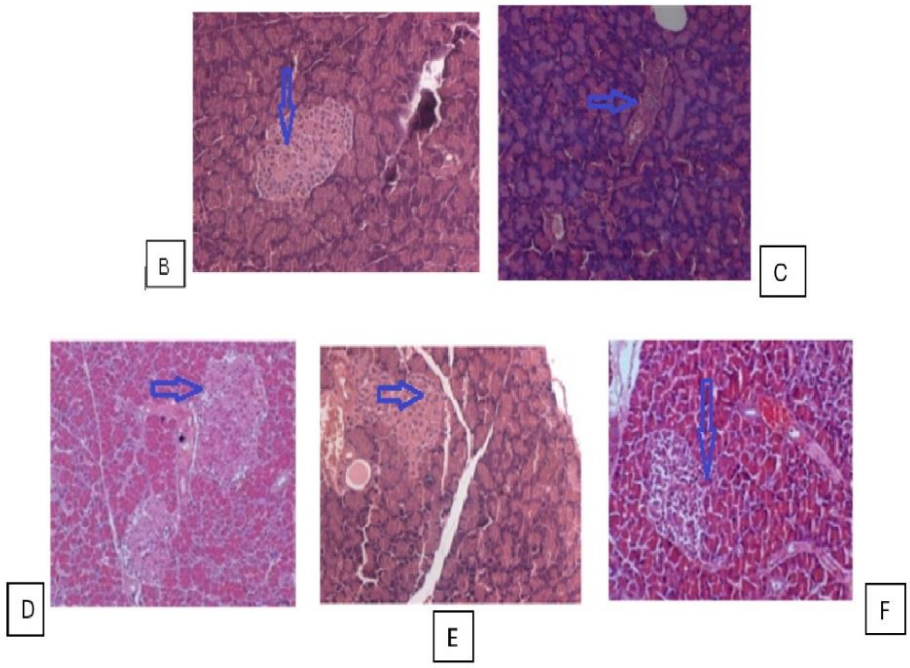

Figure 8. Effect of IMLE on lipid profile and histopathology of pancreas. (A) Lipid profile graph showing TC, HDL, LDL, VLDL, and triglycerides in experimental rats. Values are expressed as mean ± SEM, n = 6 in each group. $^{\alpha}p < 0.001$ compared to the NC group; $^{a}p < 0.001$ compared to the DC group. (B-F) Histopathological analysis of pancreas: (B) Normal control showing intact islets of Langerhans; (C) Diabetic control showing degeneration of islet cells; (D) IMLE 100 mg/kg showing moderate improvement; (E) IMLE 200 mg/kg showing regeneration of islet cells; (F) Metformin-treated group showing regeneration of islets.

$^{\alpha}p < 0.001$, $^{\beta}p < 0.01$, when compared to the NC group; $^{a}p < 0.001$, $^{b}p < 0.01$, $^{c}p < 0.05$ when compared to DC group.(Figure 8A)

3.8. Effect of IMLE on serum SGOT and SGPT levels

Diabetes induction significantly elevated serum SGOT and SGPT levels from 37 ± 1.9 U/L, 48±3.2^{a} in the NC group to 71 ± 1.6 U/L, 87 ± 2.2$^{\alpha}$ in the DC group ($^{a}p < 0.001$). Treatment with IMLE (100 and 200 mg/kg) and metformin significantly reduced both enzyme levels ($p < 0.001$) compared to the DC group, indicating a protective effect on liver function.(Table 3).

3.9. Effect of IMLE on serum antioxidant parameters

Diabetes induction dramatically lowered antioxidant defense, as evidenced by lower SOD, catalase, and GSH levels and higher MDA levels in the diabetic control (DC) group. SOD reduced from 4.9 ± 0.21 to 1.3 ± 0.037 U/mL, catalase from 8.2 ± 0.44 to 2.4 ± 0.26 kU, and GSH from 2.4 ± 0.19 to 0.32 ± 0.056 mg/dL, whereas MDA rose from 3.6 ± 0.20

Table 3. Effect of IMLE on SGOT (AST) and SGPT (ALT) levels in experimental rats

Group	Treatment	SGOT(AST) (U/L) (Mean± SD)	SGPT (ALT) (U/ L) (Mean± SD)
I	NC	37 ± 1.9	48 ± 3.2[a]
II	DC	71 ± 1.6[α]	87 ± 2.2[α]
III	IMLE 100	55 ± 1.4[a]	57 ± 1.8[a]
IV	IMLE 200	49 ± 1.6[a]	44 ± 1.2[a]
V	Standard Group	48 ± 3.2[a]	51 ± 2.5[b]

SGOT = Serum glutamate oxalaacetate transaminase; AST = Aspartate aminotransferase; SGPT = Serum glutamate pyruvate transamin ase; ALT = Alanine aminotransferase; NC = normal control, DC = diabetic control, IMLE 100 = *I.mombassana* leaf extract 100 mg/kg; IMLE 200 = *I.mombassana* leaf extract 200 mg/kg; Standard group = Metformin 100 mg/kg Values are expressed as Mean±SD (n=6).
[α]p < 0.001, [β]p < 0.01, when compared to the NC group; [a]p < 0.001, [b]p < 0.01, [c]p < 0.05 when compared to DC group.

to 9.2 ± 0.32 mg/dL. Treatment with IMLE (100 and 200 mg/kg) plus metformin substantially restored antioxidant enzyme levels and decreased MDA ($p<0.001$), showing IMLE's antioxidant efficacy against diabetes-induced oxidative stress (Table 4).

3.10. Histopathological observations

Control group: When the pancreas of control rats was examined under a microscope after H&E staining, normal cells and the rounded proportions of the Langerhans islets were seen. Prominent nuclei with well-organized lobules may be seen in Figure 8B. In pancreatic slices of untreated diabetic rats, the diabetic group showed small, shrunken islets associated with severe degenerative changes, karyolysis, reduced islet cells, congestion, and inflammatory cell infiltration (Figure.8C). Diabetes IMLE 200–400 mg, as well as the Metformin-treated group. The reversal of STZ-induced tissue damage is demonstrated in Figure 8 D, E and F wherein the pancreatic architecture returns to normal, exhibiting β-cell vacuolations, mild islet cell hyperplasia, and pancreatic parenchymal congestion. In the pancreatic tissue, lobules, islets of Langerhans, and conventional vascular and artery architecture were seen.

4. DISCUSSION

Phytochemical screening revealed that the ethanol extract of *Ipomoea mombassana* contained the highest levels of secondary metabolites, including flavonoids, tannins, saponins, and alkaloid compounds known for antioxidants, antibacterial, and antidiabetic activities. These may underline the extract's potent biological effects.

The ethanolic leaf extract exhibited strong α-amylase inhibitory activity, comparable to that of the reference drug Metformin. α-Amylase inhibitors reduce postprandial glucose levels by delaying starch hydrolysis and glucose absorption, a mechanism widely exploited in the management of type 2 diabetes. The strong inhibitory activity of IMLE may therefore be attributed to its polar bioactive constituents, particularly flavonoids and phenolic compounds, which have been consistently reported as effective enzyme inhibitors.

High-resolution LC–MS/MS analysis further demonstrated the chemical diversity of IMLE, identifying 37 metabolites belonging to several phytochemical classes. These included alkaloids (Mianserin, Pilocarpine, Abrine), terpenoids and triterpenoids (Ganoderic acid, Tephrosin, Cinncassiol A 19-glucoside), dipeptides (Valyl-Glycine, Glutamyl-Histidine), and phenolic lactones (Squamosamide, L-Rhamnono-1,4-lactone). The presence of such structurally diverse compounds is consistent with the preliminary phytochemical screening and provides a molecular basis for the biological activities observed. Although some of the most abundant chromatographic peaks (e.g., 11-amino-undecanoic acid, (S)-Edulinine) are not linked to antioxidant or antidiabetic effects, several lower-abundance metabolites such as Tephrosin, Ganoderic acid, and bioactive dipeptides have been previously reported to modulate oxidative stress and glucose metabolism. This highlights that biological activity is not necessarily correlated with chromatographic peak intensity but rather with the structural features of individual compounds.

Table 4. Effect of IMLE on Antioxidant Parameters

Parameters	NC	DC	IMLE 100	IMLE 200	Metformin group
SOD (U mL^{-1})	4.9 ± 0.21	1.3 ± 0.037[α]	5.0 ± 0.36[a]	6.2 ± 0.42[a]	6.5 ± 0.42[a]
Catalase (kU)	8.2 ± 0.44	2.4 ± 0.26[α]	6.8 ± 0.35[a]	8.9 ± 0.38[a]	8.4 ± 0.25[a]
MDA (µM)	3.6 ± 0.20	9.2 ± 0.32[α]	5.2 ± 0.19[a]	3.5 ± 0.25[a]	3.3 ± 0.28[a]
GSH (mg dL^{-1})	2.4 ± 0.19	0.32± 0.056[α]	1.5± 0.076[a]	2.6 ± 0.088[a]	2.7 ± 0.072[a]

[α]p < 0.001, [β]p < 0.01, when compared to the NC group; [a]p < 0.001, [b]p < 0.01, [c]p < 0.05 when compared to DC group.

In silico docking studies supported these findings by demonstrating strong binding affinities of key metabolites toward α-amylase, with docking scores ranging from –7.6 to –9.8 kcal/mol. Tephrosin showed the most favorable binding (–9.8 kcal/mol), forming persistent hydrogen bonds with HIS305 (74.9% occupancy) and TRP59 (52.2%). Molecular dynamics simulations confirmed the stability of this interaction, with protein RMSD stabilizing at ~0.18 nm, ligand RMSD maintained within 0.04–0.07 nm, and an average MMGBSA binding free energy of –50.73 kcal/mol over the 100 ns trajectory. These results suggest that the inhibitory activity observed *in vitro* may be mediated, at least in part, by stable molecular interactions between Tephrosin and the catalytic residues of α-amylase.

Interestingly, two compounds (Zinnimidine and Cinncassiol A 19-glucoside) were detected that have not been extensively reported in the literature, suggesting the potential for novel bioactivities and warranting further pharmacological investigation. The MS/MS fragmentation data supported the structural assignment of these metabolites, while database and literature comparisons provided additional confirmation.

Together, these findings indicate that the antidiabetic and antioxidant effects of *Ipomoea mombassana* are likely due to the combined actions of structurally diverse phytochemicals rather than a single dominant metabolite.

In vivo, STZ-induced diabetic rats treated with the ethanol extract showed reduced blood glucose levels and improved insulin secretion, indicating enhanced pancreatic β-cell function. Saponins may have contributed by promoting glucose uptake and insulin release. Additionally, the extract improved lipid profiles, likely through modulation of lipoprotein lipase activity. Hepatoprotective effects were observed, with normalization of SGOT and SGPT levels. Restoration of antioxidant enzymes (GSH, SOD, CAT) indicated reduced oxidative stress and better metabolic balance.

5. CONCLUSION

The phytochemical investigation of *Ipomoea mombassana* confirmed the presence of diverse secondary metabolites, particularly flavonoids, tannins, saponins, and alkaloids, which contribute to its pharmacological potential. *In vitro* α-amylase inhibition studies demonstrated strong enzyme inhibitory activity comparable to metformin, supporting its role in glucose metabolism regulation. HR-LC–MS/MS profiling identified 37 metabolites belonging to different phytochemical classes, including two previously unreported compounds, thereby providing a chemical basis for its broad spectrum of bioactivities. *In silico* docking and molecular dynamics simulations further validated the inhibitory potential of key metabolites such as Tephrosin, which exhibited high binding affinity and stable interactions with α-amylase catalytic residues. *In vivo* studies in STZ-induced diabetic rats revealed significant reductions in blood glucose, triglycerides, and total cholesterol levels, along with restoration of antioxidant enzyme activity and improvement in hepatic function. Collectively, these findings provide compelling evidence that *I. mombassana* possesses antidiabetic, antioxidant, antilipidemic, and hepatoprotective properties. Future research should prioritize the isolation and characterization of active compounds, mechanistic studies, and clinical trials to confirm its efficacy as a natural therapeutic candidate for diabetes management.

6. ACKNOWLEDGMENT

The authors gratefully acknowledge the management of Vels Institute of Science, Technology and Advanced Studies (VISTAS) for extending the necessary facilities to carry out this research work. This study did not receive any specific financial support from public, commercial, or not-for-profit funding organizations.

Author contribution

The author performed the experiments, analyzed the data, and prepared the manuscript. The research was conducted under the supervision of Dr.A.Vijayalakshmi, who provided guidance, reviewed the manuscript, and approved the final version.

Funding

None declared.

Conflict of interest

The authors declare no conflict of interest.

Ethics approval

All experimental procedures were conducted by the guidelines of the Institutional Animal Ethics Committee (IAEC), under approval number CCSEA/IAEC/JLS/21/04/017.

Article info:

Received April 29, 2025
Received in revise form October 31, 2025
Accepted November 8, 2025

REFERENCES

1. American Diabetes Association. Classification and diagnosis of diabetes: Standards of medical care in diabetes-2023. Diabetes Care. 2023;46(Suppl 1):S19-40.
2. Bellia A, Sbraccia P, D'Adamo M, Guglielmi V, Lombardo MF, Federici M, et al. Association between different modalities of insulin administration and metabolic dysfunction-associated fatty liver disease in adults with type 1 diabetes mellitus. Diabetes Res Clin Pract. 2023;204:110898.

3. Chen W, Sun H, Liu H, Li X, Zhang Y, Wang J, et al. Effect of recurrent severe insulin-induced hypoglycemia on cognitive function and brain oxidative status in rats. Diabetol Metab Syndr. 2024;16(1):13.
4. Verdcourt B. Convolvulaceae. In: Milne-Redhead E, Polhill RM, editors. Flora of Tropical East Africa. London: Crown agents for overseas governments and administrations; 1963.
5. Biju SD, Vajravelu E, Sabu M. *Ipomoea mombassana* (Hallier f.) Verdc. (Convolvulaceae) A new record for India from Kerala. J Econ Taxon Bot. 1998;22(3):711–2
6. Pullaiah T. Flora of Telangana-The 29th State of India. New Delhi: Regency Publications; 2015.
7. Reddy KN, Reddy CS. Flora of Telangana State, India. Dehradun: Bishen Singh Mahendra Pal Singh; 2016.
8. Mascarenhas M, Mandrekar C, Marathe P, Morais L. Phytochemical screening of selected species from Convolvulaceae. Int J Curr Pharm Res. 2017;9:94. doi:10.22159/ijcpr.2017v9i6.23438.
9. Paramesh L, Reddy VB. *Ipomoea mombassana* Vatke (Convolvulaceae)-New record to the flora of Telangana State, India. J Indian Bot Soc. 2020;100(3-4):200. doi:10.5958/2455-7218.2020.00034.0.
10. Akther R, Kabir A, Akhter S. *Ipomoea digitata*: A therapeutic boon from nature to mankind. Res J Pharm Biol Chem Sci. 2021;12(5):123-34.
11. Kumar V, Singh P, Sharma R. Phytochemical and pharmacological properties of *Ipomoea carnea*: A review. *Phytojournal*. 2021;10(1A):384-92.
12. Patel N, Joshi H, Mehta S. Phytochemical analysis of various *Ipomoea* species and their pharmacological potentials. Plants J. 2020;8(4D):249-57.
13. Sinan KI. Phytochemical screening, antioxidant, antibacterial, and α-amylase inhibitory activity of *Moringa oleifera* Lam. leaves. J Nepal Chem Soc. 2023;43(2):141-50. doi:10.3126/jncs.v43i2.53360.
14. Laaraj R, Eloutassi N. Phytochemical screening, antioxidant activity, and α-amylase inhibition study using different extracts of loquat (*Eriobotrya japonica*) leaves. BMC Chem. 2023;17:112. doi:10.1186/s13065-021-00768-9.
15. Fiehn O. Metabolomics the link between genotypes and phenotypes. Plant Mol Biol. 2002;48(1-2):155-71. doi:10.1023/A:1013713905833.
16. Wolfender JL, Marti G, Thomas A, Bertrand S. Current approaches and challenges for the metabolite profiling of complex natural extracts. J Chromatogr A. 2015;1382:136-64. doi:10.1016/j.chroma.2014.10.091.
17. Pagadala NS, Syed K, Tuszynski J. Software for molecular docking: A review. Biophys Rev. 2017;9(2):91-102. doi:10.1007/s12551-016-0247-1.
18. Vijh D, Sharma R, Mehta P, Singh A, Kaur G, Patel S, et al. GC-MS analysis, molecular docking, and molecular dynamics of *Dalbergia sissoo* antidiabetic phytochemicals. Sci Rep. 2024;14:23456. doi:10.1038/s41598-024-75570-3.
19. Jain NK, Verma P, Sharma A, Gupta R, Mehta S, Singh D, et al. Computational network pharmacology, molecular docking and molecular dynamics simulations of phytoconstituents. Pharmaceuticals. 2025;18(4):508. doi:10.3390/ph18040508.
20. Hollingsworth SA, Dror RO. Molecular dynamics simulation for all. Neuron. 2018;99(6):1129–43. doi:10.1016/j.neuron.2018.08.011.
21. Lenzen S. The mechanisms of alloxan- and streptozotocin-induced diabetes. Diabetologia. 2008;51(2):216–26. doi:10.1007/s00125-007-0881-7.
22. Kim HJ, Kim D, Yoon H, Choi CS, Oh YS, Jun HS. Prevention of oxidative stress-induced pancreatic β-cell damage by *Broussonetia kazinoki* Siebold fruit extract via the ERK-Nox4 pathway. Antioxidants. 2020;9(5):406.
23. Yang Y, Zhang JL, Shen LH, Feng LJ, Zhou Q. Inhibition of diacylated anthocyanins from purple sweet potato (*Ipomoea batatas* L.) against α-amylase and α-glucosidase. Food Chem. 2021;359:129934. doi:10.1016/j.foodchem.2021.129934.
24. Majekodunmi SO. Review of extraction of medicinal plants for pharmaceutical research. *MRJMMS*. 2015;3:521-7.
25. Hossain MA, Al-Hdhrami SS, Weli AM, Al-Riyami Q, Al-Sabahi JN. Isolation, fractionation and identification of chemical constituents from the leaves crude extracts of *Mentha piperita* L. Asian Pac J Trop Biomed. 2014;4:S368–72. doi:10.12980/APJTB.4.2014C1051.
26. Harborne JB. Phytochemical Methods: A guide to modern techniques of plant analysis. 3rd ed. London: Chapman & Hall; 1998. p. 219.
27. Mourya P, Singh G, Jain N, Gupta MK. *In-vitro* studies on inhibition of α-amylase and α-glucosidase by plant extracts of *Alternanthera pungens* Kunth. J Drug Deliv Ther. 2018;8(6-A):64–8.
28. SAIF, Indian Institute of Technology Bombay. Facilities and instrumentation. Sophisticated Analytical Instrument Facility; IIT Bombay. Available from: https://www.ircc.iitb.ac.in/saif/facilities.html.
29. Rawat R, Kant K, Kumar A, Bhati K, Verma SM. HeroMDAnalysis: An automagical tool for GROMACS-based molecular dynamics simulation analysis. Future Med Chem. 2021;13(5):447–56.
30. Guijas C, Montenegro-Burke JR, Domingo-Almenara X, Palermo A, Warth B, Hermann G, et al. METLIN: A technology platform for identifying knowns and unknowns. Anal Chem. 2018;90(5):3156–64.
31. Trott O, Olson AJ. AutoDock Vina: Improving the speed and accuracy of docking with a new scoring function, efficient optimization, and multithreading. J Comput Chem. 2010;31(2):455–61.
32. Ghosh M. Fundamentals of Experimental Pharmacology. 2nd ed. Kolkata: Scientific Book Agency; 1994. p. 158-9.
33. Akhtar N, Akram M, Daniyal M, Ahmad S. Evaluation of antidiabetic activity of *Ipomoea batatas* L. extract in alloxan-induced diabetic rats. Int J Immunopathol Pharmacol. 2018;32:2058738418814678. doi:10.1177/2058738418814678.
34. Datta A, Bagchi C, Das S, Mitra A, Pati AD, Tripathi SK. Antidiabetic and antihyperlipidemic activity of hydroalcoholic extract of *Withania coagulans* Dunal dried fruit in experimental rat models. J Ayurveda Integr Med. 2013;4:99–106. doi:10.4103/0975-9476.113880.
35. Nagy ME, Ewais EA. Protective role of *Moringa oleifera* leaves extract against streptozotocin-induced diabetic alterations in pancreatic β-cells architecture and function. Biomed Pharmacother. 2020;127:110153. doi:10.1016/j.biopha.2020.110153.